

# Applicability of Vortex Lattice Method and its Comparison with High Fidelity Tools

Sheharyar Nasir, M Tariq Javaid, M. Usman Shahid, Asad Raza, Waseeq Siddiqui, Shuaib Salamat

Department of Aerospace Engineering, Air University, Aerospace & Aviation Campus, Kamra, Pakistan

Corresponding author: Sheharyar Nasir (Email: [shehryarnasir@aerospace.pk](mailto:shehryarnasir@aerospace.pk))

**Abstract**— Vortex Lattice Method (VLM) is a potential flow theory-based solver and is well known for inviscid aerodynamics computation. The solver possesses extensive applications in aircraft conceptual design phase because of its agility. VLM models an aircraft surface by placing various trapezoidal panels to calculate lift curve slope, induced drag and  $C_p$  distribution. This study focuses on analysis of aerodynamic characteristics of the DLR-F4 wing body configuration to compute Lift coefficient, Drag coefficient and aerodynamic efficiency L/D using VLM and CFD. The results are then compared with wind tunnel test data. The results reveal that the VLM provides accurate results in a relatively shorter amount of time and a quick overview of aircraft aerodynamics. Moreover, VLM results are in close agreement with computational and experimental data at low to moderate angles of attack. However, results begin to deviate at high angles of attack due to attached flow assumption in VLM solver.

**Keywords**— Analytical Solver; CFD; DLR-F4; Vortex Lattice Method (VLM); Wing induced Drag; Wind-tunnel

## I. INTRODUCTION

Low fidelity tools, like (VLM, PANAIR and other Panel Methods) are used in the early conceptual design phase, where a lot of different design configurations have to be tried and tested. This method is very useful in the conceptual design phase of aircraft for the fast computation of aerodynamic forces and its derivatives to get a rough qualitative overview of aircraft's aerodynamic performance. [1]. VLM method has proven to be very practical and versatile theoretical tool for the aerodynamic analysis and design of planar or non-planar configuration[2]. Vortex lattice method (VLM) applies potential flow- technique to analytically resolve aerodynamic forces[3]. It is used for solving irrotational, inviscid, and linearized flow problems about the lifting surfaces in subsonic regime using the Prandtl-Glauert equation [4]. The VLM was first introduced in the 1930's and it was also one of the first methods to be implemented on computers[5]. A 3-D configuration is simplified to a 2-D geometry by disregarding its thickness. It divides the lifting surfaces into trapezoidal panels and distributes vorticity singularities over them [6]. Thin airfoil theory is implemented to simulate and satisfy flow tangency conditions. The boundary conditions are applied on mean camber surface. Numerous equations are solved in parallel for each panel to calculate induced drag and moment. Leading edge thrust along with vortex lift effects are computed using suction parameter based on Polhamus Suction analogy.

## II. VLM BASED SOLVER

VLM is a Potential flow based solver, where the wing is simulated by multiple horseshoe vortices having varying circulation strengths  $\Gamma$  distributed on a lattice. Geometry is discretized into trapezoidal panels as shown in Fig. 1. A horseshoe vortex is placed on each panel with its bound leg on quarter chord and trailing legs along inboard and outboard

chord that extends to infinity[7]. The velocity of each vortex is measured at  $\frac{3}{4}$  chord of each panel to quantify vortex strength using flow tangency boundary condition[7].

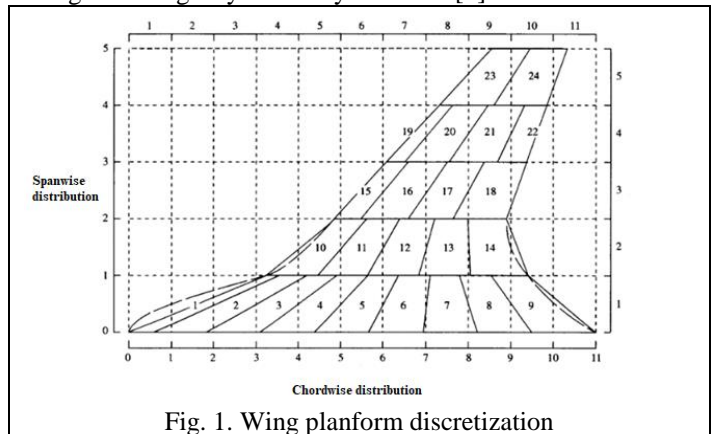


Fig. 1. Wing planform discretization

The downwash velocity created by vortex at any location on the surface of wing geometry is computed using Eq. (1)

$$\left(\frac{w}{U}\right) = \frac{\beta}{4\pi} \bar{R} \Delta u c_e \quad (1)$$

where,

- $w$  Downwash velocity
- $U$  Free stream velocity
- $\beta$  Compressibility correction factor
- $\bar{R}$  Subsonic influence function
- $\Delta u$  Longitudinal perturbation velocity difference across wing surface
- $c_e$  Element average chord

The downwash induced by the complete wing at any location in the downstream plane of the wing can be found by the summation of effects generated by individual panel. The

downwash velocity of field element having tangency flow condition is computed at the control point using Eq. (2):

$$\left(\frac{w}{U}\right)^* = \frac{\beta}{4\pi} \overline{R^*} \Delta u^* c_e^* + \frac{\beta}{4\pi} \sum \overline{R} \Delta u c_e \quad (2)$$

where, \* represents field element.

Flow tangency boundary condition derived from thin airfoil theory is given by Eq. (3):

$$\left(\frac{w}{U}\right)^* = \left(\frac{dz}{dx}\right)^* \quad (3)$$

where,

$$\left(\frac{dz}{dx}\right) \quad \text{Slope of mean camber at control point}$$

Perturbation velocity difference for field element is estimated by Eq. (4) as

$$\Delta u^* = \frac{4\pi}{\beta} \frac{1}{\overline{R^*} c_e^*} \left(\frac{dz}{dx}\right)^* - \frac{1}{\overline{R^*} c_e^*} \sum \overline{R} \Delta u c_e \quad (4)$$

Pressure coefficients are obtained from perturbation velocities using linearized theory assumption given by Eq. (5)

$$\Delta C_p^* = 2\Delta u^* \quad (5)$$

where,

$$\Delta C_p \quad \text{Lifting pressure coefficient}$$

As pressure coefficient is a linear function of perturbation velocity difference, therefore, its contribution for camber and flat wing can be added by superposition. Hence, the results from VLM based solver for other angles of attack are obtained by combining the solution of input cambered wing ( $\alpha=0^\circ$   $\alpha = 0^\circ$ ) with the results of flat wing having the same planform ( $\alpha=1^\circ$ ). The correlation of section leading edge thrust coefficient for flat wing is given by Eq. (6)

$$C_{t,f} = \left(\frac{\sin \alpha}{\sin 1^\circ}\right)^2 \frac{\pi}{2} \frac{b}{S_{ref}} \sqrt{\tan \Lambda_{L,E}^2 + \beta^2} \times \left[(\Delta u \sqrt{x'})_{o,f}\right]^2 \quad (6)$$

where,

$$C_{t,f} \quad \text{Coefficient of Section leading edge thrust for flat wing}$$

$$b \quad \text{Wing span}$$

$$S_{ref} \quad \text{Wing reference area}$$

$$\Lambda_{L,E} \quad \text{Leading edge sweep angle}$$

$$(\Delta u \sqrt{x'})_{o,f} \quad \text{Leading edge singularity parameter for flat wing}$$

The section leading edge thrust for cambered wing is related to thrust coefficient for flat wing and is given as in Eq. (7)

$$C_t = C_{t,f} \left(\frac{\sin \alpha - \sin \alpha_{zt}}{\sin 1^\circ}\right)^2 \quad (7)$$

Where,

$$C_t \quad \text{Section leading edge thrust coefficient for cambered wing}$$

$$\alpha_{zt} \quad \text{Zero thrust angle of attack}$$

Polhamus Suction analogy relates leading edge thrust coefficient with vortex force coefficient [3] as given in Eq. (8)

$$C_{vor} = \frac{C_t - C_{t,a}}{\cos \Lambda_{L,E}} \quad (8)$$

Where,

$$C_{t,a} \quad \text{Attainable section leading edge thrust coefficient}$$

$$C_{vor} \quad \text{Vortex force coefficient}$$

Pressure coefficient is converted into section normal and axial force coefficients which are integrated over the wing surface and are related to angle of attack to determine coefficient of lift and coefficient of induced drag as given by Eqs. (9) and (10)

$$C_L = C_N \cos \alpha - C_A \sin \alpha \quad (9)$$

$$C_{D,i} = C_N \sin \alpha + C_A \cos \alpha \quad (10)$$

### III. METHODOLOGY

The geometric specifications of DLR-F4 wing used in this study are given in Table I[8]. Analysis is performed using analytical, computational and wind tunnel technique.

Table I: Geometric specifications

Wing Span	1.2 m
Mean Aerodynamic chord	0.14 m
Aspect ratio	9.3
Airfoil	Customized [9]
Taper ratio	0.49
Wing reference area	0.15 m <sup>2</sup>
Leading edge sweep	27 <sup>o</sup>
Dihedral angle	+4 <sup>o</sup>

The flight conditions used in this study are given in Table II.

Table II: Flight conditions

Mach	0.75
Altitude	Sea-level

#### A. Wind Tunnel

Redeker conducted experiments on DLR-F4 in three different test facilities [10] using flight conditions given in Table II. The test facility capabilities are given in Table III as:

Table III: Specifications of Wind Tunnel test facility

Facility	DRA, Bedford UK	NLR, Amsterdam	ONERA S2MA, France
Test Section dimensions	2.44m x 2.44m	2m x 1.60m	1.77m x 1.75m
Type	Pressurized Subsonic/Supersonic	HST High speed wind tunnel	----

Aerodynamic forces were computed for various angles of attack at  $3 \times 10^6$  Reynold number. ONERA S2MA test facility data is taken for comparison.

*B. Computational Fluid Dynamics*

Computational fluid dynamics (CFD) uses Navier–Stokes equations to numerically solve fluid flow problems [11]. Pirzadeh and Frink[12] performed the CFD analysis of DLR-F4 geometry using Spalart-Allmaras one-equation model in USM3Dns solver. In the current study, CFD analysis is performed using commercial ANSYS fluent solver. A cylindrical domain of length 20 times and radius 15 times the length of fuselage encapsulates the DLR-F4 model as shown in Fig. 2.

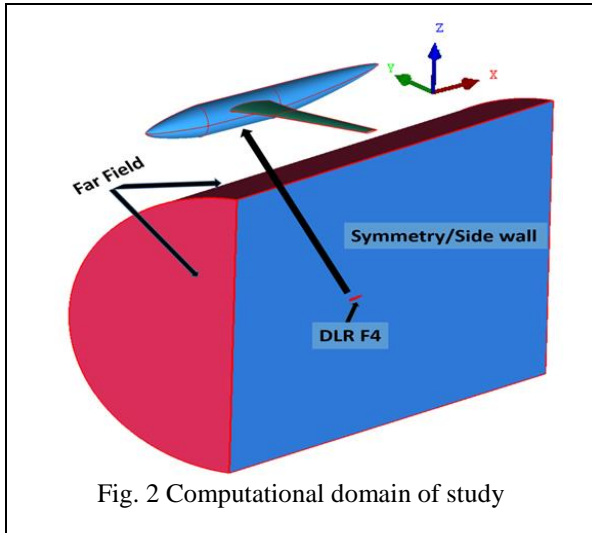


Fig. 2 Computational domain of study

The model is subtracted from the domain in order to create volume between the domain surface and the DLR-F4 model. The geometry is imported to the grid generator. Unstructured grids composed of tetrahedral, triangle, and prism elements are generated using ANSYS ICEM. The expansion ratio of the volume from the models is set to 1.25. Total 18 prism layers are used to capture the boundary layer with first cell height of  $6\mu\text{m}$ . This is done to ensure that the non-dimensional wall distance ( $y^+$ ) is set below 1.0. The overall size of grid consists of 14 million elements and 5 million nodes. Flight condition

and boundary conditions used in CFD simulations are tabulated in Table IV and Table V.

Table IV: Simulation details

Angle of attack	-4 to 10
Mach number	0.75
Mesh Size	14 Million

Table V: Boundary conditions

Far field	Gauge Pressure = 101 kPa
	Temperature = 288 K
Operating Conditions	Pressure (0 Pa)
DLR-F4 surface	Wall
Side wall	Symmetry

The surface mesh of DLR-F4 wing and volume mesh of domain is shown in Fig. 3 and Fig. 4.

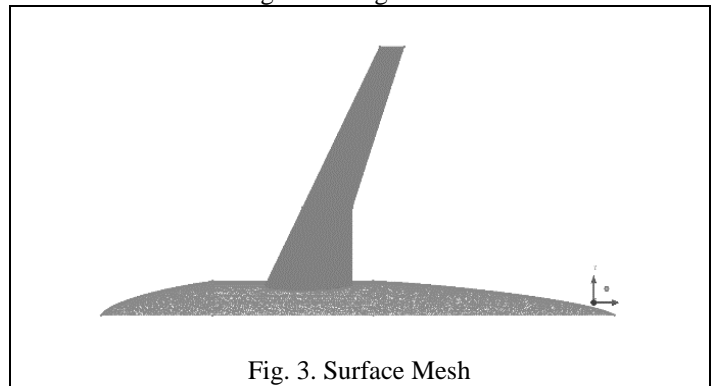


Fig. 3. Surface Mesh

A single block unstructured grid comprising of tetrahedral cells was generated for Navier-Stokes (RANS) computations. Advancing-front and the advancing-layers techniques are utilized for grid generation. Both techniques resemble marching procedures by which tetrahedral cells grow in the computational field from a triangular surface mesh (initial front). The advancing process continues until the entire domain is filled with contiguous tetrahedral cells.

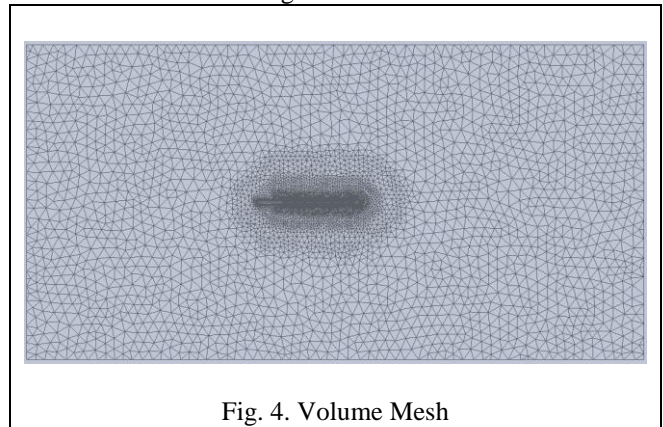


Fig. 4. Volume Mesh

The time averaging of all the terms in Navier-Stoke's equations (known as RANS) results in turbulence stress. It needs to be modeled through turbulence models for achieving closure using Boussinesq's hypothesis. Several different turbulence models exist. Out of them, SST-K $\omega$  is used which captures near wall effects as well as far field effects[13]. 2<sup>nd</sup> order accurate spatial discretization schemes and pressure-velocity coupled schemes have been used in the analysis.

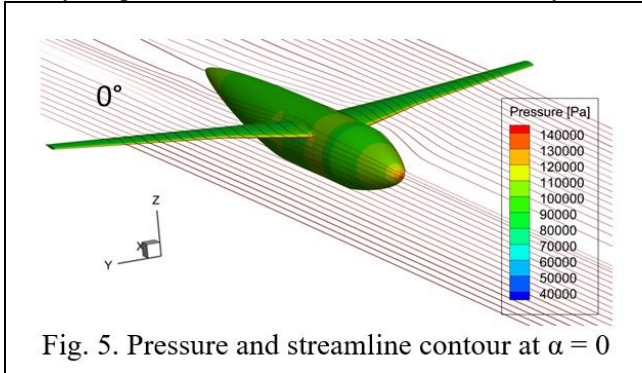


Fig. 5. Pressure and streamline contour at  $\alpha = 0$

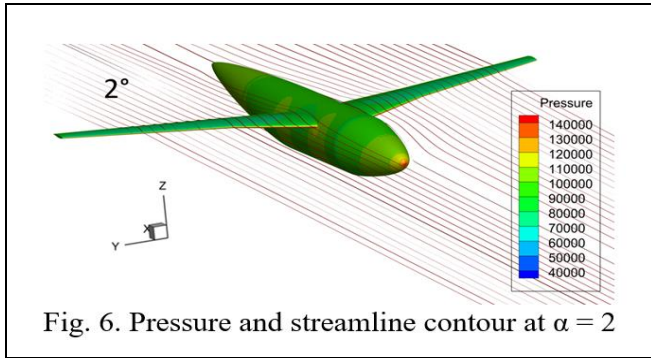


Fig. 6. Pressure and streamline contour at  $\alpha = 2$

Figure 5 to Fig. 8 show the pressure and streamline contours at various angles of attack. Streamlines behavior in Fig. 7 shows that flow tends to detach at 6-degree angle of attack. The wing root stalls at 10-degree angle of attack and flow becomes fully detached from the upper surface of the wing as shown in Fig. 5 to Fig. 8. Pressure and streamline contour at  $\alpha = 0^\circ$ .

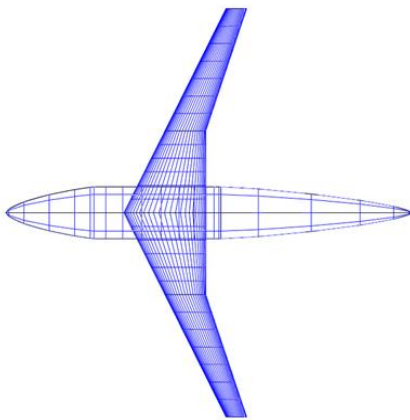


Fig. 9. Open VSP geometry for VLM based solver

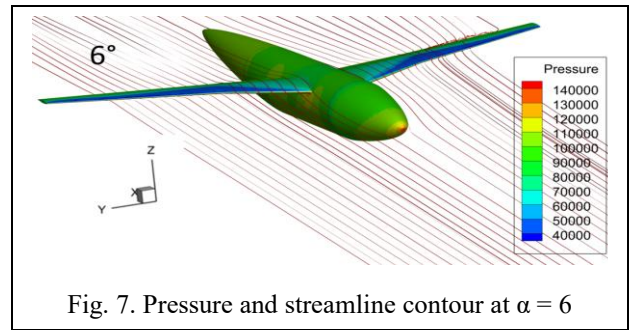


Fig. 7. Pressure and streamline contour at  $\alpha = 6$

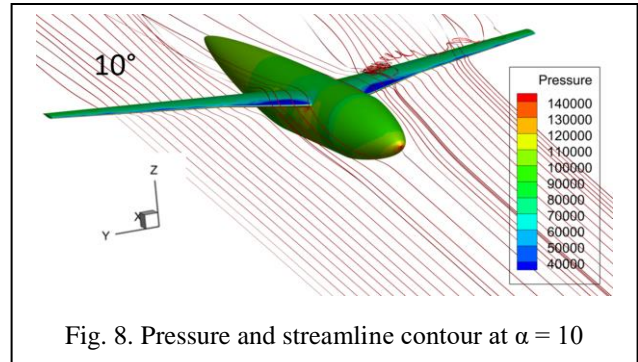


Fig. 8. Pressure and streamline contour at  $\alpha = 10$

### C. Vortex Lattice Method

A wing-body is generated using Open VSP with dimensions given in Table I and is shown in Fig. 9.

Wing-body geometry is divided along the span and chord using parameters JBYMAX and ELAR to generate the panels. This geometry is imported to the solver in .txt format. The solver is executed under above mentioned flight conditions and an output file is generated. This file contains the geometric characteristics and aerodynamic coefficients that incorporate the effects of leading edge thrust and vortex lift. The process flowchart for VLM computation is shown in Fig. 10.

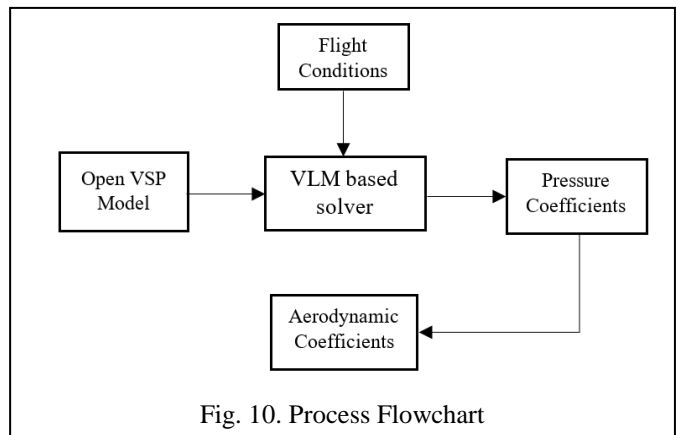


Fig. 10. Process Flowchart

#### IV. RESULTS & DISCUSSION

CFD and extended VLM based solver results for coefficient of lift vs. angle of attack are plotted in Fig. 11.

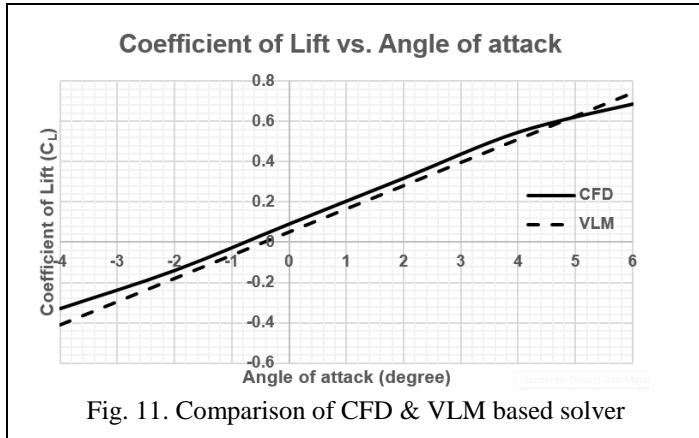


Fig. 11. Comparison of CFD & VLM based solver

The flow begins to detach at 6-degree angle of attack from the wing shown in Fig. 5 and VLM results tend to deviate from CFD results at 6-degree angle of attack due to the attached flow assumption.

Wind Tunnel data [9], CFD and extended VLM based solver results for drag polar are plotted in Fig. 12. Zero lift drag coefficient for DLR-F4 is taken from Wind tunnel data and is merged with VLM based solver results. It can be seen that CFD results are in proximity with Wind tunnel results. It implies the accurate estimation of boundary layer effects. Coefficient of lift and induced drag, given by VLM based solver, are over-estimated at high angles of attack because of treating the flow to be attached.

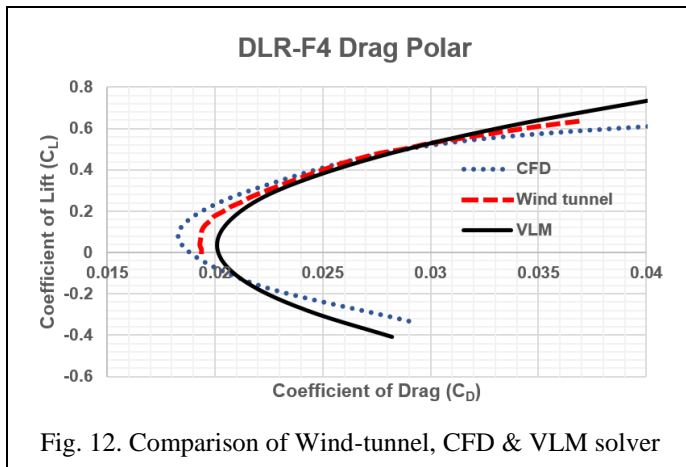


Fig. 12. Comparison of Wind-tunnel, CFD & VLM solver

#### V. CONCLUSION

In this study, aerodynamic coefficients from VLM based solver are compared to Wind Tunnel and CFD. Results of VLM, a potential flow solver, are found in close agreement with Wind Tunnel and CFD at low to moderate ( $0^\circ$  to  $5^\circ$ ) angles of attack. The maximum percentage error in lift coefficient from VLM comes out to be 11% as compared to CFD in low to moderate range of angles of attack. Wind tunnel experimentation and CFD are cost intensive in design optimization stage. Hence, it is recommended to use VLM based solver for reasonable prediction.

#### REFERENCES

- [1] Schindler, J.P.W., *Feasibility study of different methods for the use in aircraft conceptual design*. 2012.
- [2] Miranda, L.R., R.D. Elliot, and W.M. Baker, *A generalized vortex lattice method for subsonic and supersonic flow applications*. 1977.
- [3] Simpson, R.J., R. Palacios, and J. Murua, *Induced-drag calculations in the unsteady vortex lattice method*. AIAA journal, vol. 51, no. 7: p. 1775-1779, 2013.
- [4] Mason, W.H., *Applied Computational Aerodynamics*. 1997.
- [5] Administration, N.A.A.S., *Vortex-Lattice Utilization*. January 1, 1976 Langley Research Center Hampton, Virginia.
- [6] H.W. Carlson, R.J.M., *Studies of Leading-Edge Thrust Phenomena*. AIAA (American Institute of Aeronautics and Astronautics), 1980.
- [7] Septiyana, A., et al. *Analysis of aerodynamic characteristics using the vortex lattice method on twin tail boom unmanned aircraft*. in *AIP Conference Proceedings*. 2020. AIP Publishing LLC.
- [8] Redeker, G., *DLR-F4 Wing-Body Configuration*. AGARD-AR-303, 1994. 2: p. II.-.
- [9] J.C. Vassberg, P.G.B., C.L. Rumsey, *Drag Prediction for DLR-F4 Wing-body using OVERFLOW and CL3D on an overset mesh*. AIAA (American Institute of Aeronautics and Astronautics), 2002.
- [10] Redeker, G., *DLR-F4 wing-body configuration - A Selection of Experimental Test Cases for the Validation of CFD Codes*. 1994.
- [11] Karansinghdangi, M.N.m., *CFD Analysis of an Aircraft delta wing*. International Research Journal of Engineering and Technology(IRJET), vol. 03, no. 12, 2016.
- [12] Pirzadeh, S. and N. Frink. *Assessment of the unstructured grid software TetrUSS for drag prediction of the DLR-F4 configuration*. in *40th AIAA Aerospace Sciences Meeting & Exhibit*. 2002.
- [13] Lacombe, F., D. Pelletier, and A. Garon. *Compatible wall functions and adaptive remeshing for the k-omega SST model*. in *AIAA Scitech 2019 Forum*. 2019.